

LA-4186

DIC-15 REPORT COLLECTION
REPRODUCTION
COPY

C.B.

LOS ALAMOS SCIENTIFIC LABORATORY
of the
University of California
LOS ALAMOS, NEW MEXICO

Curves for Predicting Stresses
in Controlled Fusion
Pulsed Magnetic Field Systems



UNITED STATES
ATOMIC ENERGY COMMISSION
CONTRACT W-7405-ENG 36

LEGAL NOTICE

This report was prepared as an account of Government sponsored work. Neither the United States, nor the Commission, nor any person acting on behalf of the Commission:

A. Makes any warranty or representation, expressed or implied, with respect to the accuracy, completeness, or usefulness of the information contained in this report, or that the use of any information, apparatus, method, or process disclosed in this report may not infringe privately owned rights; or

B. Assumes any liabilities with respect to the use of, or for damages resulting from the use of any information, apparatus, method, or process disclosed in this report.

As used in the above, "person acting on behalf of the Commission" includes any employee or contractor of the Commission, or employee of such contractor, to the extent that such employee or contractor of the Commission, or employee of such contractor prepares, disseminates or provides access to, any information pursuant to his employment or contract with the Commission, or his employment with such contractor.

This report expresses the opinions of the author or authors and does not necessarily reflect the opinions or views of the Los Alamos Scientific Laboratory.

Printed in the United States of America. Available from
Clearinghouse for Federal Scientific and Technical Information
National Bureau of Standards, U. S. Department of Commerce
Springfield, Virginia 22151

Price: Printed Copy \$3.00; Microfiche \$0.65

Written: May 23, 1969

Distributed: September 25, 1969

LA-4186

UC-20, CONTROLLED

THERMONUCLEAR PROCESSES

TID-4500

LOS ALAMOS SCIENTIFIC LABORATORY
of the
University of California
LOS ALAMOS • NEW MEXICO

Curves for Predicting Stresses
in Controlled Fusion
Pulsed Magnetic Field Systems

by

D. A. Baker

L. W. Mann



TABLE OF CONTENTS

	Page
I. Introduction	1
II. Theory	1
A. Model	1
B. Equation of Motion	1
C. General Solution	2
D. Damped Sinusoid Magnetic Field	2
E. Magnetic Field with a Sinusoidal Rise and Exponential Decay	3
III. Results	4
A. General	4
B. Description of the Use of the Curves	4
IV. Sample Problems	12
A. Parallel-Plate Transmission Line	12
B. Quadrupole Current Rings	14
Appendix: Impulse Approximation	16
Design Curves	
Impulse Factor for Damped Sinusoid Magnetic Field	6
Impulse Factor for Crowbarred Magnetic Field Waveform	7
Mechanical Response for Oscillatory Waveform	8
Mechanical Response for Crowbarred Waveform	10

CURVES FOR PREDICTING STRESSES IN CONTROLLED FUSION PULSED MAGNETIC FIELD SYSTEMS

by

D. A. Baker and L. W. Mann

ABSTRACT

A set of curves is given to aid in the prediction of an elastic system response to the impulsive magnetic forces commonly encountered in controlled fusion research. Results for two magnetic field waveforms are given, (1) an exponentially damped sinusoid, and (2) a sinusoidal rise-to-peak field followed by an exponential decay corresponding to the application of a "crowbar" to sustain the field.

I. INTRODUCTION

The design of the current rings for the Los Alamos Scientific Laboratory (LASL) Quadrupole Injection Experiment motivated this work. These rings must withstand the large impulsive forces resulting from the associated pulsed high magnetic field. Because the design of structures to withstand these forces is a frequent problem in controlled thermonuclear research (CTR), especially at LASL, we believed it worthwhile to record the results of our studies as a set of curves. These curves aid in the prediction of maximum stresses arising in pulsed magnetic field systems that are energized from capacitive energy storage banks.

II. THEORY

A precise calculation of the stresses in systems encountered in CTR work would involve solving systems of three-dimensional, elastic wave equations with appropriate driving terms and boundary conditions. Although such an ambitious calculational program may be possible with present electronic computers, we have restricted ourselves here to a vastly simplified model.

A. Model

The mechanical system is treated as a mass (e.g., a coil or transmission line plate) constrained by an elastic member (e.g., bolts or clamps) and driven by a time-dependent force proportional to the square of the magnetic field.

The motion is treated as one-dimensional and the mass is lumped, i.e., the total mass is assumed to move as a unit, and motions associated with other degrees of freedom (buckling, elastic waves, etc.) are suppressed. We neglect all effects that result in mechanical damping, because those effects are usually unknown. This approximation gives a conservative design since mechanical damping lowers the stresses actually obtained.* Our model corresponds to a driven, simple harmonic oscillator shown schematically in Fig. 1.

B. Equation of Motion

From Newton's laws, the equation of motion for the system shown in Fig. 1 is

$$m d^2x/dt^2 + kx = f(t), \quad (1)$$

or

$$d^2x/dt^2 + \omega^2 x = f(t)/m, \quad (1a)$$

where m is the mass being accelerated,

$$\omega = \sqrt{k/m}, \quad (2)$$

is the natural frequency of oscillation of the

*The experimental work of Sawyer and Zimmerman,¹ in which measurements were made of the deflection of the collector plates of the Los Alamos Scylla IA theta pinch, shows that such systems have a high Q. Consequently, a design based upon the zero mechanical damping is not greatly overconservative.

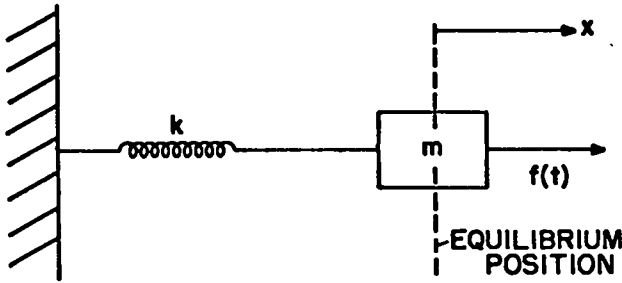


Fig. 1. Driven simple harmonic oscillator model of the elastic system.

mechanical system, and k is the effective spring constant defined so that the elastic restoring force is given by

$$f_{\text{elastic}} = -kx \quad (3)$$

The forcing function $f(t)$ is the total force applied to the mass by the magnetic field, and the variable x is the displacement from the equilibrium position. It is convenient to introduce dimensionless variables so that the resulting solutions will be in dimensionless form, which reduces the number of graphs required to display the results. We introduce two normalizing constants whose values will characterize the forcing function for each case treated later. These constants are a force f_m and a time interval τ . We then define the normalized displacement and time as

$$X = kx/f_m, \quad T = t/\tau. \quad (4)$$

Substituting into Eq. (1), we obtain

$$\frac{d^2 X}{dT^2} + \Omega^2 X = F(T), \quad (5)$$

where the normalized frequency and forcing function are given by

$$\Omega = \omega\tau, \quad (6)$$

and

$$F(T) = \Omega^2 f(\tau T)/f_m. \quad (7)$$

C. The General Solution

We obtain a general quadrature solution for Eq. (5) by using the Laplace transform method.²

Transforming to the Laplace variable s for the system initially at rest [$x(0) = \dot{x}(0) = 0$], we obtain

$$s^2 \bar{X}(s) + \Omega^2 \bar{X}(s) = \bar{F}(s),$$

where the bars denote the transformed function.

Solving for $\bar{X}(s)$, we have

$$\bar{X}(s) = \bar{F}(s)/(s^2 + \Omega^2).$$

We now inverse transform using

$$\mathcal{L}^{-1}\{\bar{F}(s)\} = F(T),$$

$$\mathcal{L}^{-1}\left\{\frac{1}{s^2 + \Omega^2}\right\} = \frac{\sin \Omega T}{\Omega},$$

$$\mathcal{L}^{-1}\{\bar{F}_1(s) \bar{F}_2(s)\} = \int_0^T f_1(\lambda) f_2(T - \lambda) d\lambda$$

(convolution formula),

and obtain the solution for X as

$$X(T) = \frac{1}{\Omega} \int_0^T F(\lambda) \sin[\Omega(T - \lambda)] d\lambda. \quad (8)$$

This is the expression for ratio of the displacement from equilibrium at any time to that caused by a constant force f_m . We next evaluate this expression for two prescribed functions $F(T)$.

D. Damped Sinusoid Magnetic Field

The first magnetic field waveform we shall treat is sketched in Fig. 2 and is given by

$$B = B_0 e^{-T/\tau_d} \sin(2\pi T/\tau), \quad (9)$$

which is a damped oscillatory waveform commonly

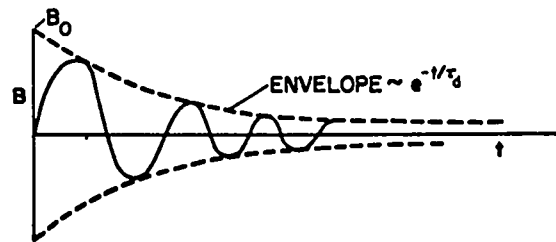


Fig. 2. Field waveform for a damped oscillatory circuit.

encountered in pulsed CTR experiments. The associated total force will be proportional to the square of the field

$$f(t) = f_m e^{-2t/\tau_d} \sin^2(2\pi t/\tau) . \quad (10)$$

This expression defines the characteristic quantities, f_m and τ , used for normalization in Section II.B. Here f_m is the peak force corresponding to the undamped field, and τ is the field period.

Substituting Eqs. (7) and (10) into Eq. (8) we have

$$X(T) = \Omega \int_0^T e^{-2\lambda\tau/\tau_d} \sin^2(2\pi\lambda) \sin[\Omega(T - \lambda)] d\lambda .$$

The integral is readily evaluated by making use of the identity

$$\sin x = \frac{1}{2}(e^{ix} - e^{-ix})$$

to replace the trigonometric functions in the integrand. With these substitutions, the integrand is of the form

$$\text{Integrand} = (i/8) \sum_{j=1}^6 c_j e^{A_j + B_j \lambda} ,$$

which can be readily integrated to give our desired result.

$$X(T) = (i\Omega/8) \sum_{j=1}^6 \frac{c_j e^{A_j}}{B_j} \left(e^{B_j T} - 1 \right) , \quad (11)$$

where

$$\begin{aligned} A_1 = A_2 = A_3 = i\Omega T, & \quad A_4 = A_5 = A_6 = -i\Omega T, \\ B_1 = a + i(4\pi - \Omega), & \quad B_2 = a - i\Omega, \\ B_3 = a - i(4\pi + \Omega), & \quad B_4 = a + i(4\pi + \Omega), \\ B_5 = a + i\Omega, & \quad B_6 = a - i(4\pi - \Omega), \end{aligned}$$

with

$$a = -2\tau/\tau_d,$$

and

$$C_1 = C_3 = 1, C_2 = -2, C_4 = C_6 = -1, C_5 = 2 .$$

E. Magnetic Field with a Sinusoidal Rise and Exponential Decay

The second field waveform we shall treat is one that is encountered when an oscillatory circuit is crowbarred at the time of peak field. The ideal-

ized* magnetic-field waveform is shown in Fig. 3 and is described by

$$B(t) = B_0 \sin 2\pi t/\tau \quad t \leq \tau/4 , \quad (12)$$

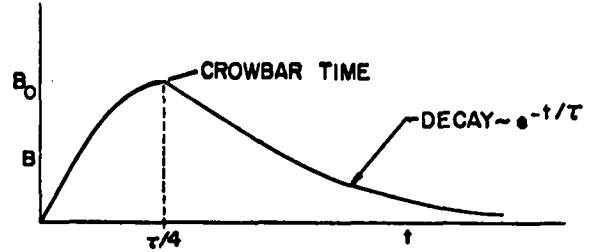


Fig. 3. Idealized waveform for a passive crowbar.

and

$$B(t) = B_0 e^{-(t-\tau/4)/\tau_d} \quad t \geq \tau/4 \quad (13)$$

The corresponding forcing function is

$$f(t) = f_m \sin^2(2\pi t/\tau) \quad t \leq \tau/4, \quad (14)$$

$$= f_m e^{-2(t-\tau/4)/\tau_d} \quad t \geq \tau/4. \quad (15)$$

The normalizing constants f_m and τ correspond to the peak force on the system and to the total period associated with the sinusoidal rise of the field. Substituting Eqs. (7), (14), and (15) into Eq. (8) yields

$$\begin{aligned} X(T) &= \Omega \int_0^T \sin^2(2\pi\lambda) \sin[\Omega(T - \lambda)] d\lambda \\ &= \Omega \int_0^{\tau/4} \sin^2(2\pi\lambda) \sin[\Omega(T - \lambda)] d\lambda \\ &\quad + \Omega \int_{\tau/4}^T e^{-2(\lambda-\tau/4)\tau/\tau_d} \sin[\Omega(T - \lambda)] d\lambda \end{aligned} \quad \begin{aligned} T &\leq 1/4, \\ T &\geq 1/4. \end{aligned}$$

Expanding $\sin[\Omega(T - \lambda)]$ using the trigonometric identity for sum of angles yields integrals that are readily evaluated analytically. When this is done, the desired formula results.

* We neglect the damping for the first rise and the oscillatory modulation of the decaying part of the waveform that occurs in actual circuits. These effects can be compensated for to some extent by a proper choice of the constants B_0 and τ_d if the true waveform is known.

$$X_1(T) = \left(\frac{1}{2}\right) \left\{ \frac{\Omega^2 (\cos 4\pi T - \cos \Omega T)}{(4\pi)^2 - \Omega^2} + (1 - \cos \Omega T) \right\} \quad (16)$$

for $T \leq 1/4$ and $\Omega \neq 4\pi$,

$$X_1(T) = \frac{1}{2} \{ 1 - 2\pi T \sin 4\pi T - \cos 4\pi T \} \quad (17)$$

for $T \leq \frac{1}{2}$ and $\Omega = 4\pi$, and

$$X_2(T) = \frac{X_1(\frac{1}{2}) + \Omega^2 \left[\exp(-2\tau T/\tau_d) + \tau/2\tau_d \right] + (2/\Omega)(\tau/\tau_d) \sin \Omega(T - \frac{1}{2}) - \cos \Omega(T - \frac{1}{2})}{(2\tau/\tau_d)^2 + \Omega^2} \quad (18)$$

for $T > \frac{1}{2}$. We use the subscripts 1 and 2 to denote the solution before and after crowbar time.

III. RESULTS

A. General

For a given mechanical system, the stress in any supporting members (the spring in our model) will be proportional to the displacement. Thus, $X(T)$, which is the ratio of the displacement $X(t)$ due to magnetic forces to the displacement $x_m = f_m/k$ that would be caused by a constant force f_m , is also the ratio of the corresponding stresses resulting from these forces. Therefore, once the function $X(T)$ is known, we need only to calculate the static stress corresponding to the maximum force f_m and to multiply the result by $X(T)$. If the system is prestressed (is in a stressed state while in the equilibrium position), this stress must be added algebraically to the result to determine if the total stresses are acceptable (under the yield stress).

The results, as obtained by computer evaluation, of Eqs. (11), (16), (17), and (18) are displayed in two forms.

1. A set of curves to be used in design applications that show the maximum stress* in units corresponding to the static force associated with the maximum value of the undamped field.
2. A selected set of curves that show the time history of the normalized stress (or displacement), $X(T)$.

* This maximum stress was obtained by a direct search on the computer because it has no simple analytic formula. The usual technique of setting the time derivative to zero would involve solving transcendental equations. In addition, the system is oscillatory and there are many relative maxima and minima. The largest relative maximum has to be sorted out.

ment), $X(T)$. The latter curves are given to show the rather complex waveforms of the resulting mechanical vibrations.

B. Description and Use of the Curves

In the past, LASL designed systems to withstand the stresses corresponding to the peak value of the magnetic field when treated as constant in time.

For short pulses, this is a conservative procedure because the ignored inertial effects will reduce the resulting effectiveness of the force. As the systems at LASL became more demanding, this over-conservative estimate became too restrictive and a procedure was adopted to reduce the design stress from the above static stress estimate by a factor, which we call the impulse factor, to take advantage of the inertial forces. The impulse factor normally used was 0.25 and was based on a single experiment conducted by Dike.³ However, the allowable impulse factor depends both upon the mechanical properties of the system and upon the field pulse duration and shape. Figures 4 and 5 allow prediction of the impulse factor for the two common field waveforms. Figure 4 gives the impulse factor (the maximum value of the displacement or stress ratio, $X(T)$, defined earlier) for a damped sinusoidal magnetic field, and Fig. 5 gives the corresponding factor for the crowbarred case. The impulse factor is plotted as a function of τ_m/τ , (the ratio* of the mechanical period $2\pi/\omega$ to the full period associated with the sinusoidal part of the waveform) with τ/τ_d as a parameter. The quantity τ_d is the time constant (e-folding time) associated with the exponential component of the waveform. Thus, to obtain an impulse factor for a given situation, one must first determine the effective mechanical period of the system

$$\tau_m = 2\pi\sqrt{m/k}, \quad (19)$$

where m is the mass to be set in motion, and k is the effective spring constant. The determination

* This ratio is related to Ω which appears in Eqs. (11), (16), and (18), i.e., $\tau_m/\tau = 2\pi/\Omega$.

of τ_m normally is where most of the labor is involved. The quantities τ and τ_d are determined once the field waveform to be used is known. Then the appropriate set of curves with the dimensionless ratios τ_m/τ and τ/τ_d is entered and the impulse factor from the ordinate is read. To calculate absolute stresses, the usual static stress (calculated to correspond to the peak field force) is then multiplied by the impulse factor and the prestress, if any, is added.

The curves of Figs. 4 and 5 show that the impulse factor can range from zero to infinity for the damped sinusoid case, and from zero to a factor of two for the crowbarred case. The most stringent case for the former occurs when the mechanical frequency is in resonance with the fundamental frequency of the forcing function, i.e., when τ_m is half the magnetic field period. The lesser peaks in Figs. 4 and 5 correspond to resonances at other frequencies in the Fourier spectrum of the forcing function. The crowbarred waveform can yield stresses higher than those predicted by the usual static stress calculation when the total magnetic field rise time is short and its decay time is long, as compared with the mechanical period of the system. The regions below the dotted lines on the curves

show where a formula obtained with the impulse approximation [where $f(t)$ is approximated by a Dirac delta function $F_0\delta(t)$ with $F_0 = \int_0^\infty f(t)dt$] gives agreement to within 5%. The derivations of the impulse approximation formulas given in the captions of Figs. 4 and 5 are given in the appendix. These formulas can be used when the impulse factors are too small to appear on the graphs.

Figures 6 and 7 show the effect of varying τ_m/τ with τ/τ_d fixed at unity. The parameters are arranged in order of increasing τ_m/τ . Only enough stress vs time curves are shown to give a general idea of the complexity of the mechanical response. The time history of the stress or displacement for any given set of parameters can be obtained by running the computer program.

There is one characteristic of strength of materials that may aid in reducing the criticality of a design for pulsed systems: Under pulsed load conditions, the yield strengths of most materials increases appreciably over that measured under static loading conditions. This bonus is offset to some extent by the phenomenon of fatigue which can make a system fail after many pulsed loads have been applied.

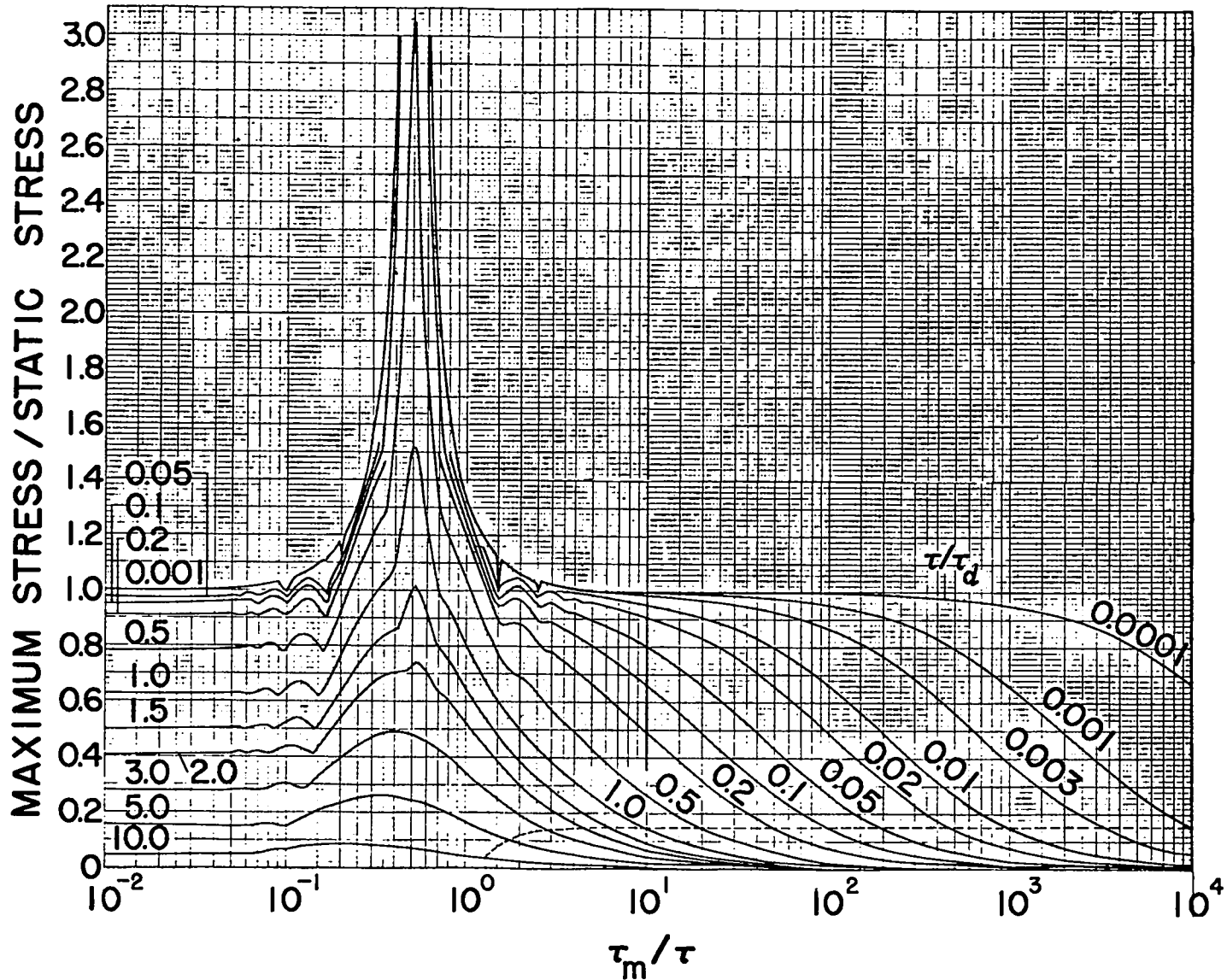


Fig. 4. Impulse factor for a damped sinusoid magnetic field. Below the dashed line, the impulse approximation formula is within 5%.

Impulse formula:
$$S_{\max}/S_{\text{static}} = \frac{2}{(\tau/\tau_d)(\tau_m/\tau)} \left[\frac{\pi^3}{(\tau/\tau_d)^2 + 4\pi^2} \right]$$

Symbols: τ = full period of the magnetic field, τ_d = e-folding constant of the damping, and τ_m = period of the mechanical system.

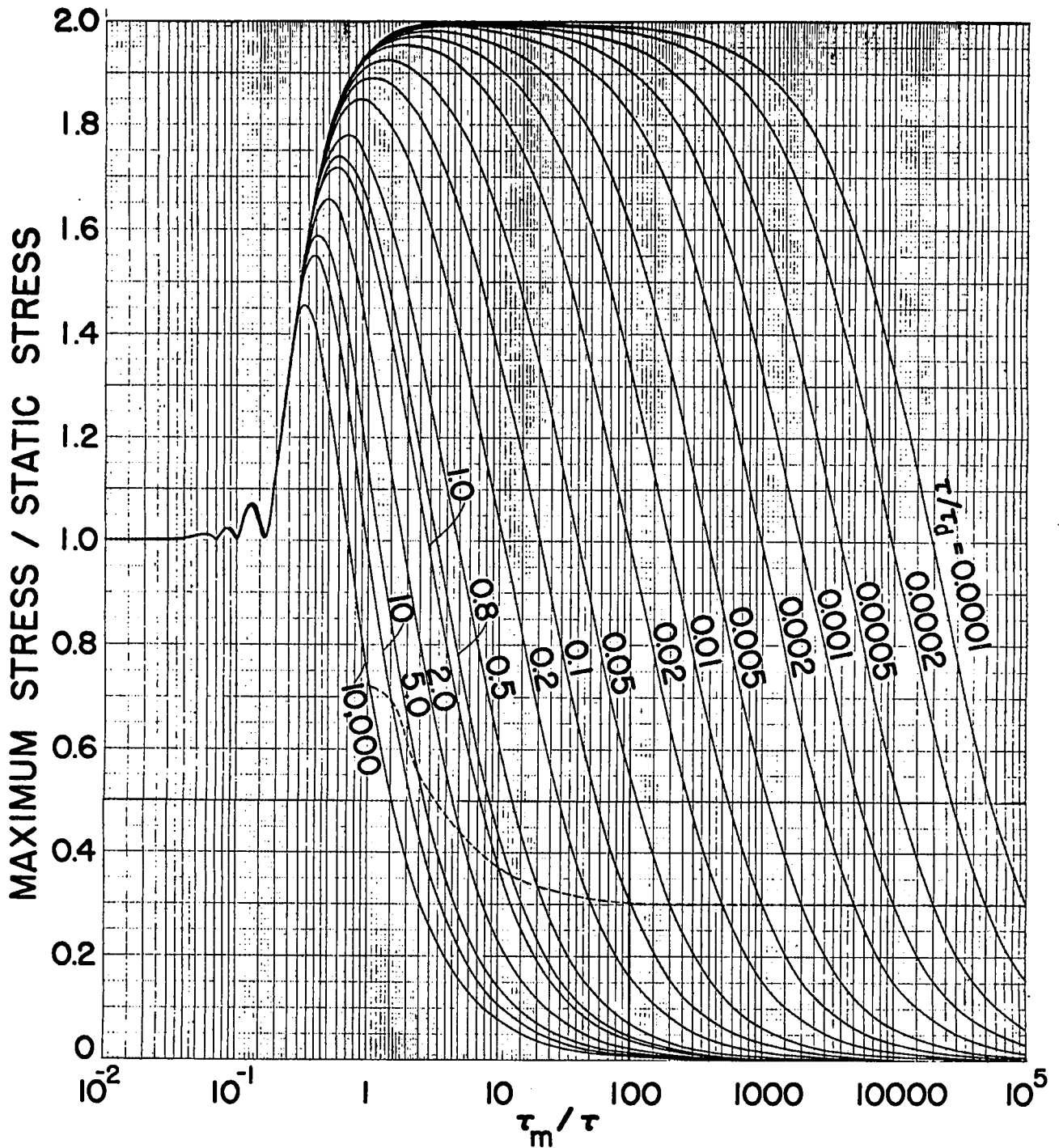


Fig. 5. Impulse factor for a crowbarred magnetic field waveform. Below the dashed line, the impulse approximation formula

$$S_{\max} / S_{\text{static}} = \frac{\pi}{(\tau_m / \tau)} [k + \tau_d / \tau]$$

is within 5%. Symbols: τ = full period associated with the rise of the field, τ_d = e-folding time of the waveform after crowbar time and τ_m = mechanical period of the system.

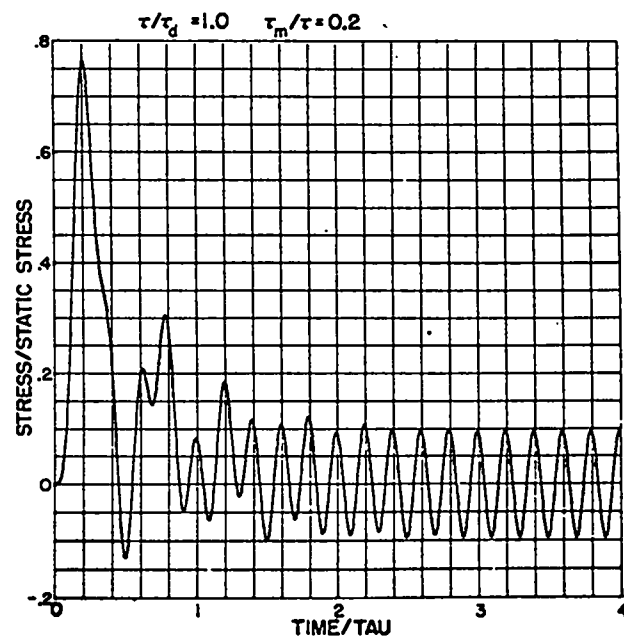
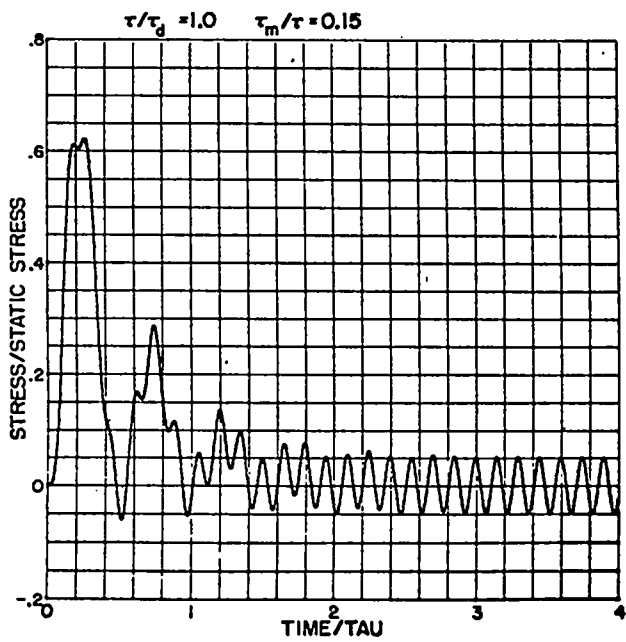
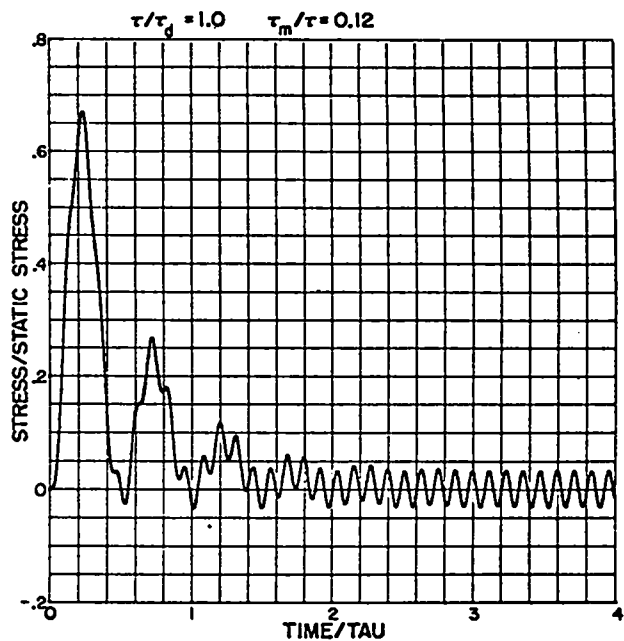
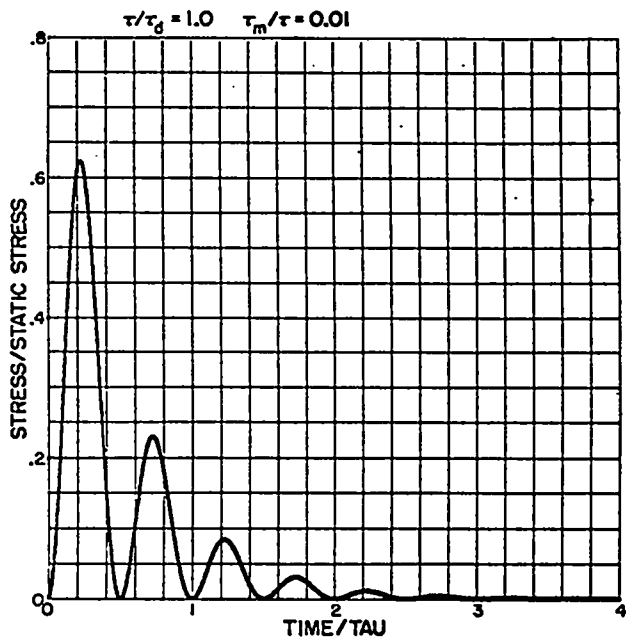


Fig. 6. Response curves (deflection or stress vs time) of an elastic system driven by the forces corresponding to a damped sinusoidal magnetic field.

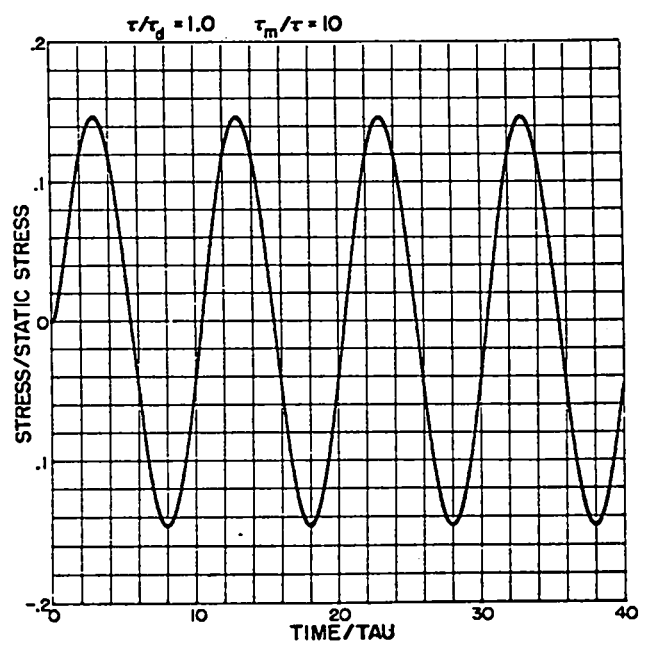
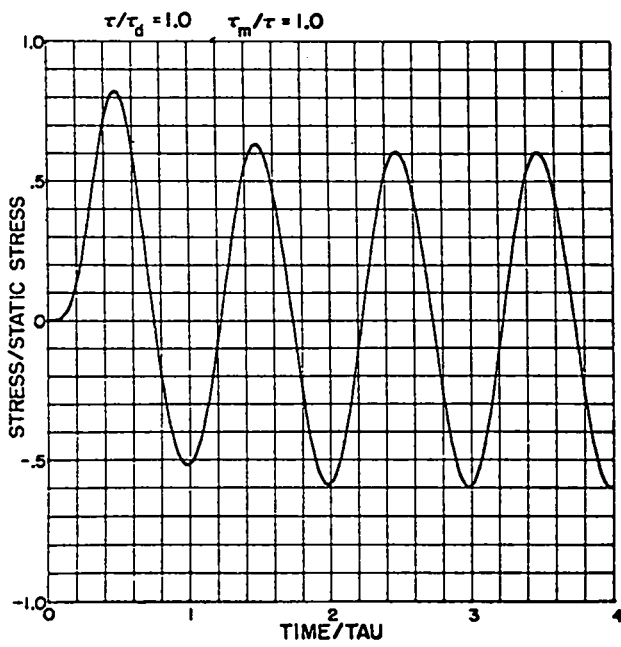
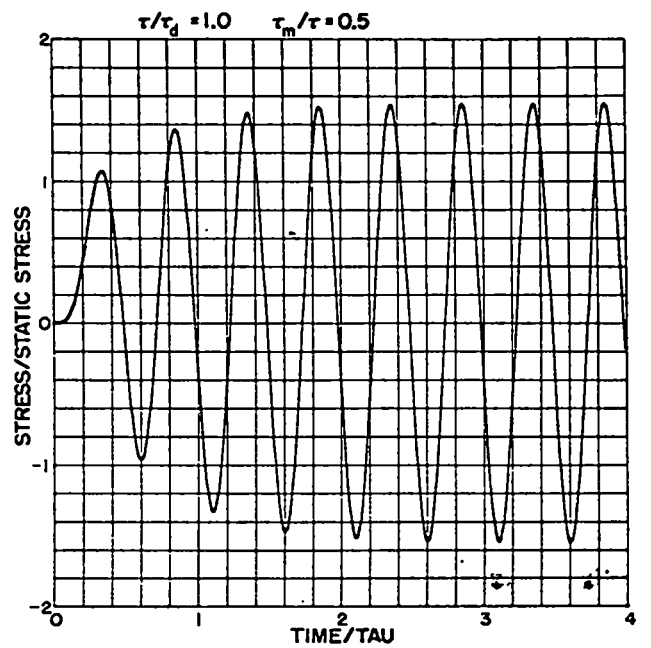
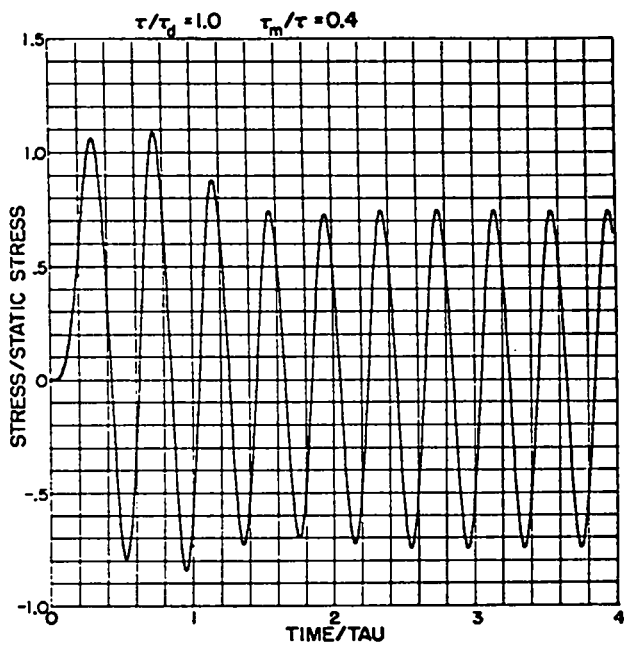


Fig. 6. Cont.

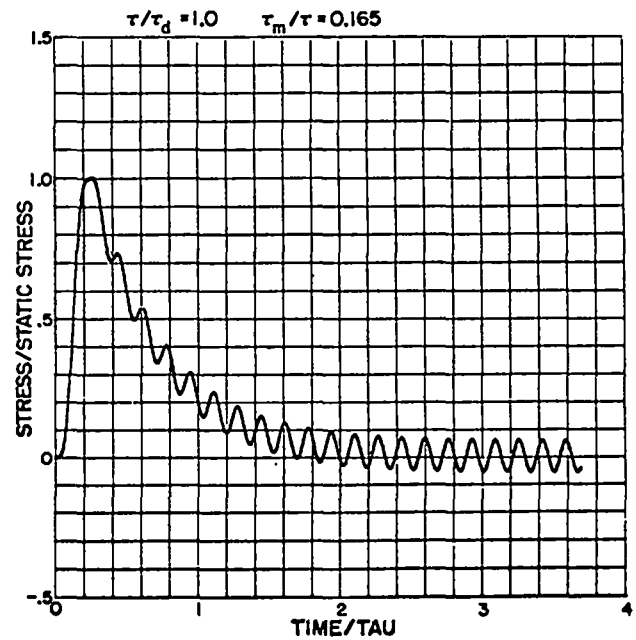
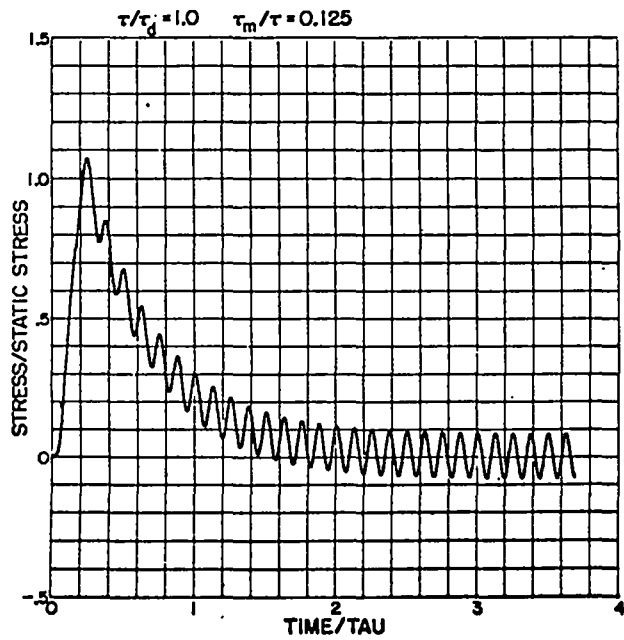
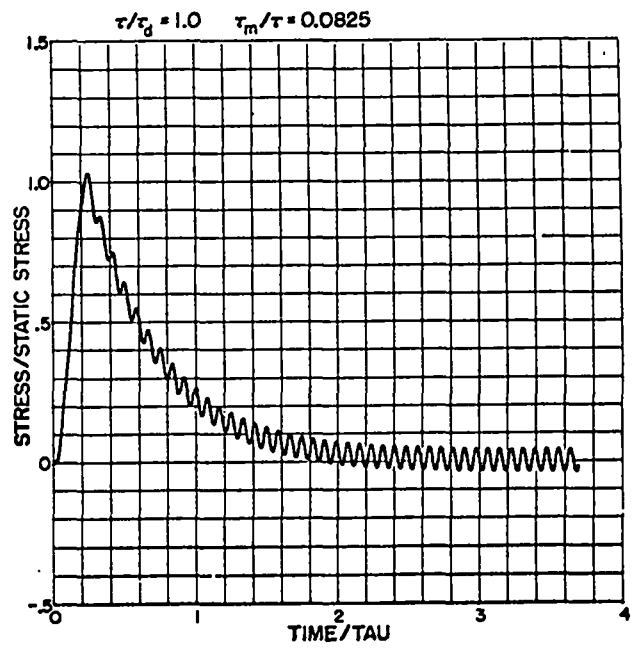
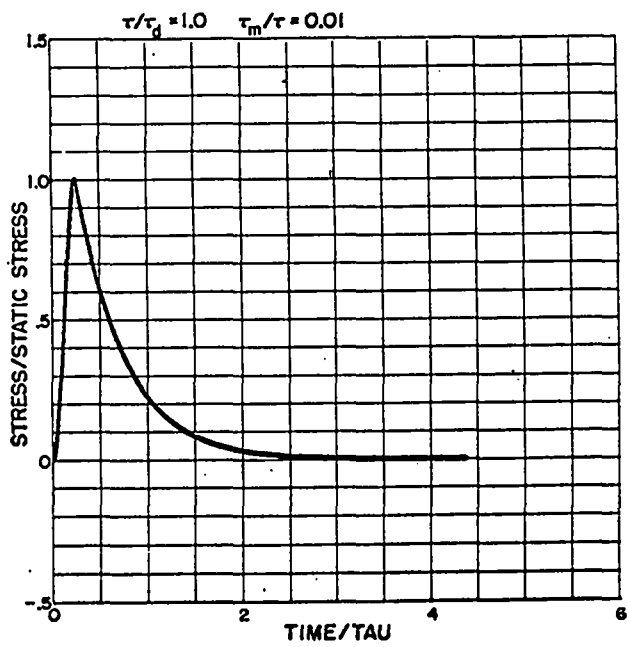


Fig. 7. Response curves of an elastic system driven by the forces associated with crowbarred magnetic field waveform.

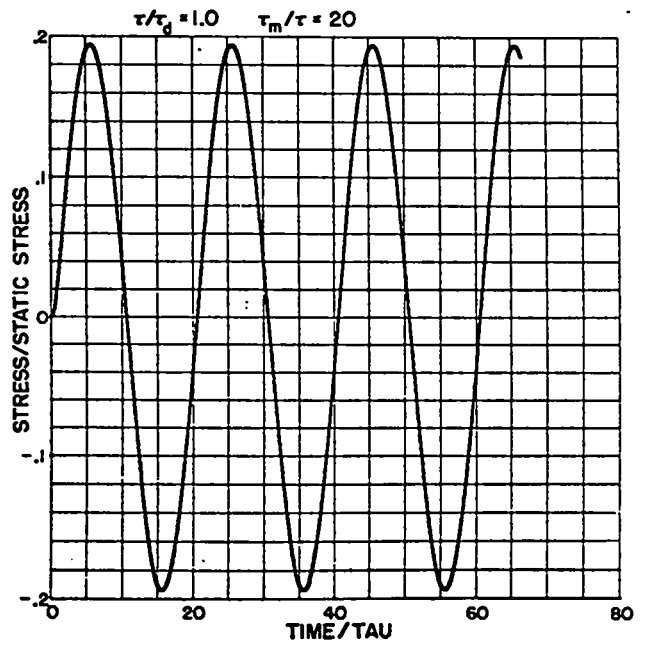
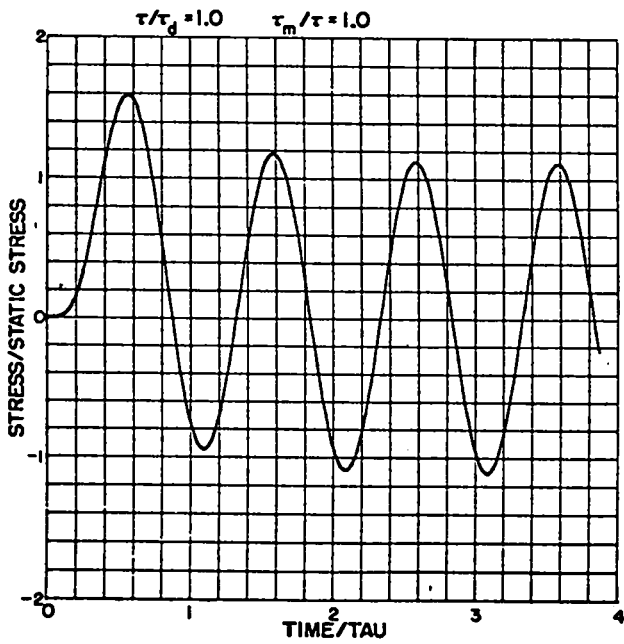
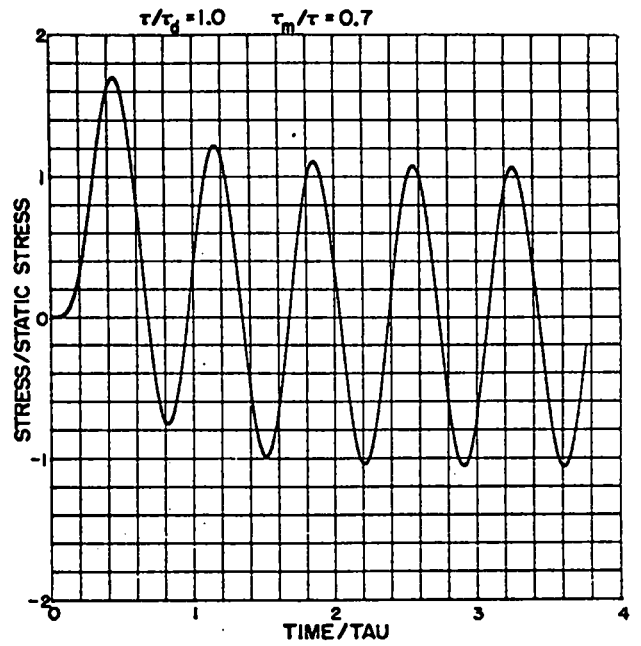
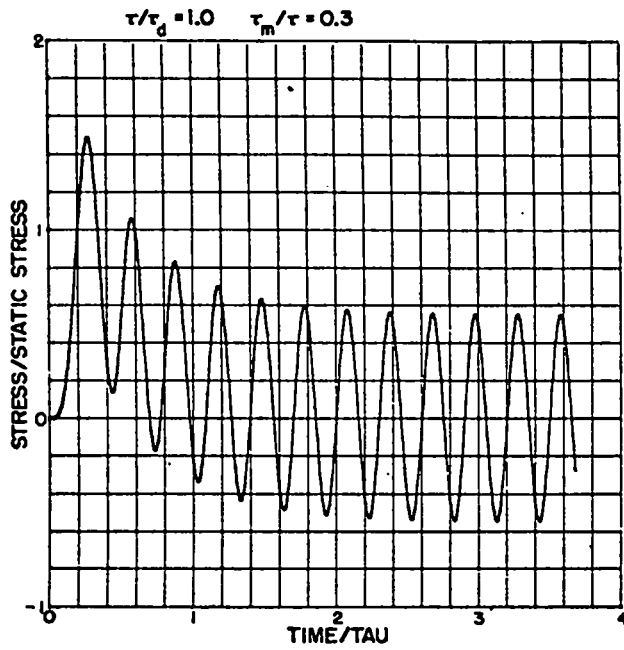


Fig. 7. Cont.

IV. SAMPLE PROBLEMS

A. Parallel-Plate Transmission Line

The design of a high-current transmission line to withstand large impulsive magnetic field forces is a problem commonly encountered in controlled thermonuclear research. As an example of how the curves may be used, we shall treat the following problem.

Problem:

An aluminum parallel-plate transmission line (plate thickness = 4 in.) is uniformly held with insulated through bolts, one for every 100 sq in. of plate. The plates are separated by 0.060 in. of Mylar insulation and the bolts are prestressed and supported on thick nylon insulating cylinders as shown in Fig. 8. For the dimensions given in Fig. 8, what is the minimum preload force that must be

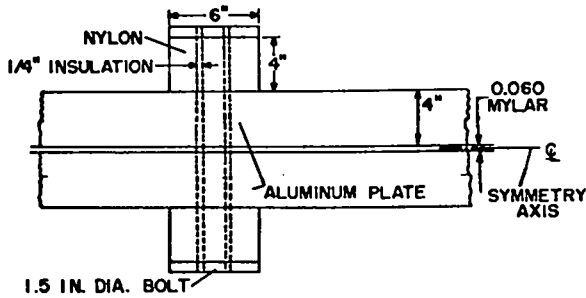


Fig. 8. Transmission line section for the first sample problem.

applied to each bolt so that the plates never leave the Mylar insulation when the magnetic field between the plates rises sinusoidally to 20 kG in 2 μ sec, and decays exponentially in 1 msec (crow-barred waveform)? By what amount is the force of tension in each bolt increased by the field pulse under the above conditions?

Solution:

1. Preliminary Assumptions. We assume that the magnetic field is uniform and we neglect the field fringing effects. We further treat the motion of the plates as a whole and ignore any plate flexing between the bolts. We consider the system on a section-per-bolt basis because mass, force, and spring constants are additive quantities for a parallel system. The mechanical period and the deflection is the same whether it is treated on a section-per-bolt or on a total-plate basis.

2. Model. The first step is to set up an equivalent spring mass system (Fig. 9). The symmetry axis in the Mylar is motionless, therefore we can treat each half of the line as a separate identical system. We treat the plate as the total lumped mass and ignore its compressibility. The bolt, nylon, and Mylar are treated as a compound spring system with spring constants k_B , k_N , and k_M .

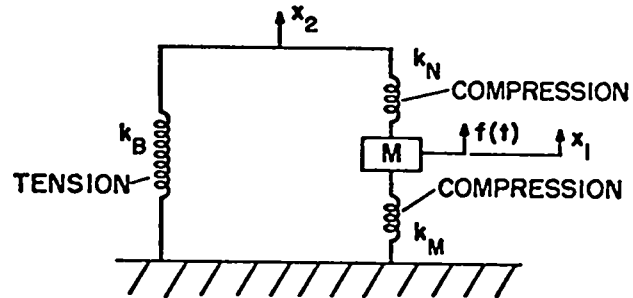


Fig. 9. Equivalent spring system. x_1 and x_2 are the displacements of the plate and bolt head from the equilibrium positions.

3. Reduction to an Equivalent System. We first reduce the compound system to the simple system of Fig. 1 for which the theory applies. Systems of springs in parallel, or in series, are equivalent to a single spring system with an effective spring constant, k_{eff} . In such cases, the effective spring constant of the system can be obtained by treating the individual spring constants like conductances, i.e., for springs in series

$$\frac{1}{k_{eff}} = \frac{1}{k_1} + \frac{1}{k_2} + \dots + \frac{1}{k_n}, \quad (20)$$

and for springs in parallel

$$k_{eff} = k_1 + k_2 + \dots + k_n. \quad (21)$$

In a given compound spring system, if how to proceed is doubtful, the equations of motion for the model system can be written and then, by substitution, all of the displacement variables can be eliminated except for the lumped mass. From the resulting equation, the effective spring constant will be evident. We now apply this procedure to the system of Fig. 9. From Newton's laws,

$$m d^2 x_1 / dt^2 = -k_M x_1 - k_N (x_1 - x_2) + f(t), \quad (22)$$

and

$$k_B x_2 = k_N (x_1 - x_2). \quad (23)$$

Solving Eq. (23) for x_2 gives

$$x_2 = \frac{k_N}{k_N + k_B} x_1. \quad (24)$$

We substitute Eq. (24) into Eq. (22) and obtain

$$m d^2 x_1 / dt^2 + \left[k_M + \frac{k_N k_B}{k_N + k_B} \right] x_1 = f(t). \quad (25)$$

Comparing Eq. (25) with Eq. (1), we see that the effective spring constant for the system is

$$k_{\text{eff}} = k_M + \frac{k_N k_B}{k_N + k_B}, \quad (26)$$

showing that the elastic system consists of a series connection of the bolt and nylon acting in parallel with the Mylar.

4. Computation of the Effective Spring Constant.

The spring constant for a cylinder of material (not necessarily circular) with Young's modulus E , cross-sectional area A , and length ℓ is given by

$$k = EA/\ell. \quad (27)$$

We shall use values of E of 29×10^6 , 35×10^4 , and 5×10^5 psi for the steel bolt, nylon, and Mylar, respectively. Taking dimensions from Fig. 8, we obtain

$$k_B = \frac{(2.9 \times 10^7) \pi (0.75)^2}{8} = 6.41 \times 10^6 \text{ lb/in.}$$

$$k_N = \frac{(3.5 \times 10^5) \pi (3^2 - 1^2)}{4} = 2.20 \times 10^6 \text{ lb/in.}$$

$$k_M = \frac{(5 \times 10^5)(100)}{(0.030)} = 1.67 \times 10^9 \text{ lb/in.}$$

$$k_{\text{eff}} = 1.67 \times 10^9 + \frac{(6.41 \times 10^6)(2.20 \times 10^6)}{6.41 \times 10^6 + 2.20 \times 10^6}$$

$$= 1.67 \times 10^9 + 1.65 \times 10^6 \text{ lb/in.}$$

$$= 1.67 \times 10^9 \text{ lb/in.}$$

Here we see the dominance of the Mylar spring constant due to its large area and small thickness.

5. Calculation of the Mass Set in Motion. We shall neglect the mass of the bolt and the nylon as compared to the plate. For a density ρ of aluminum of 0.0975 lb/in.^3 we obtain

$$\begin{aligned} m &= (\rho/g) \times \text{Volume} \\ &= \frac{(0.0975 \text{ lb/in.}^3)(4 \text{ in.} \times 100 \text{ in.}^2)}{(386 \text{ in./sec}^2)} \\ &= 0.101 \text{ lb-sec}^2/\text{in.} \end{aligned}$$

6. Calculation of the Mechanical Period.

$$\begin{aligned} \tau_m &= 2\pi\sqrt{m/k_{\text{eff}}} \\ &= 2\pi\sqrt{0.101 \text{ lb-sec}^2/\text{in.} / 1.67 \times 10^9 \text{ lb/in.}} \\ &= 48.9 \text{ } \mu\text{sec}. \end{aligned}$$

7. Calculation of the Impulse Factor. A rise time of $2 \text{ } \mu\text{sec}$ corresponds to $\tau = 8 \text{ } \mu\text{sec}$. From the problem statement, $\tau_d = 1 \text{ msec}$. We compute the required dimensionless quantities

$$\tau_m/\tau = 48.9/8 = 6.11$$

$$\tau/\tau_d = 8/1000 = 8 \times 10^{-3}$$

Entering Fig. 5 with these parameters, we obtain an impulse factor of $X_{\text{max}} = 1.95$.

8. Calculation of Static Force in the Bolt Corresponding to the Peak Magnetic Field.

To convert the magnetic field to pressure, we use the fact that pressure $\propto B^2$ and that 5 kG corresponds to one atmosphere of pressure on a conductor carrying a surface current. The force on 100 cm^2 of the plate corresponding to 20 kG is

$$f_m = (20/5)^2 \times 14.7 \text{ psi} \times 100 \text{ in.}^2 = 23,520 \text{ lb.}$$

9. Calculation of Required Preloading. If the plate is not to leave the Mylar,* the resulting

* If the plate leaves the Mylar, the spring constant would change abruptly to the value corresponding to the bolt and the nylon in series. Since the curves were generated assuming spring constants that do not vary with time, they would no longer apply. An attempt is made to design such systems³ so that the insulation between the plates is never totally decompressed. This has two desirable features, (1) the plates do not slap and damage the insulation, and (2) the bolts do not cycle through a large stress range thus reducing fatigue.

displacement of the plate under the pulsed load must not be more than that caused by the initial preloading of the bolt. Letting $f(t) = f_m$ and setting $d^2x_1/dt^2 = 0$ in Eq. (25), we first solve for x_{1m} the deflection of the plate due to a static force f_m .

$$x_{1m} = f_m/k_{\text{eff}} = 23,520/(1.67 \times 10^9) \\ = 1.41 \times 10^{-5} \text{ in.}$$

The maximum displacement of the plate for the pulsed field is therefore

$$x_{1 \text{ max}} = X_{\text{max}} x_{1m} = (1.95)(1.41 \times 10^{-5}) \\ = 2.75 \times 10^{-5} \text{ in.}$$

Equating this to the deflection of the plate, due to preloading the bolt $x_{\text{preload}} = f_{\text{preload}}/k_M$, we can solve for the minimum preload required.

$$f_{\text{preload}} = (1.67 \times 10^9)(2.75 \times 10^{-5}) \\ = 45,900 \text{ lb/bolt .}$$

We see that, since the impulse factor was obtained near the maximum of the curves of Fig. 5, its value can be reduced if the mass of the plate is either reduced or increased by an appropriate amount.

10. Calculation of Peak Bolt Loading. We can calculate the maximum increase in the bolt loading due to the magnetic forces by using Eq. (24)

$$f_{\text{peak}} = k_B x_{2 \text{ max}} = \left(\frac{k_N k_B}{k_N + k_B} \right) x_{1 \text{ max}} \\ = (1.64 \times 10^6)(2.75 \times 10^{-5}) \\ = 45.1 \text{ lb/bolt .}$$

Thus the bolt experiences a negligible increase over its static preload as asserted in item 9.

B. Quadrupole Current Rings

An application of the curves arose in the design of the LASL pulsed quadrupole injection experiment. We further demonstrate the use of the curves by predicting the peak stresses due to a symmetric mode deformation in the current-carrying ring con-

ductors under crowbarred and noncrowbarred conditions.

1. Derivation of the Natural Period of Radial Oscillations of a Thin Ring. We consider a differential element of a thin ring (the cross-sectional radial dimension is small compared to the major radius) as shown in Fig. 10.

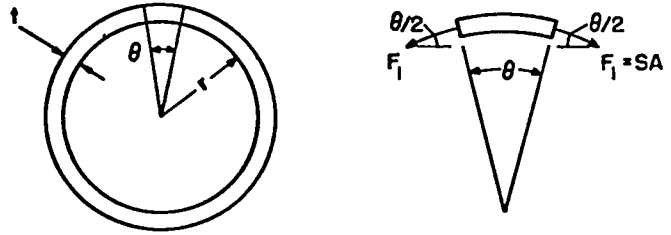


Fig. 10. Schematic and free body diagram for the thin ring of the second sample problem.

A radial displacement of the ring with cross-sectional area, A, by an amount Δr gives rise to tangential stresses, S, as follows

$$S = E \text{ Strain} = E(\Delta l/l) = E(\Delta r/r), \quad (28)$$

where E is Young's modulus. From the free-body diagram of Fig 8, the resulting radial restoring force, F, is given by

$$F = 2F_1 \sin(\theta/2) = 2SA \sin(\theta/2) \\ \approx SA\theta \text{ (for small } \theta) .$$

Inserting the expression for S,

$$F = (EA\theta/r)\Delta r \equiv k\Delta r,$$

so that the spring constant is seen to be

$$k = EA\theta/r . \quad (29)$$

The mass of the element is

$$m = M\theta/2\pi,$$

where M is the total mass of the ring. The natural period for radial oscillations of the ring is therefore

$$\tau_m = \sqrt{2\pi m/k} = \sqrt{2\pi Mr/EA} = \sqrt{2\pi Wr/gEA} , \quad (30)$$

where

W = total weight of the ring,
r = mean major radius,
g = acceleration of gravity,
A = ring cross-sectional area, and
E = Young's modulus.

Equation (20) may also be written in a more convenient form

$$\tau_m = 2\pi r \sqrt{E/\rho} = \frac{\text{circumference}}{\text{sound speed}} \quad (31)$$

where ρ is the mass density, so that τ_m is the transit time of a compressional wave once around the ring.

2. Numerical Results for the LASL Quadrupole

Design.

a. Calculation of the Mechanical Period. The parameters for the two concentric aluminum coils used in the LASL Quadrupole design are as follows

	<u>Inner Coil</u>	<u>Outer Coil</u>
Radius r	18.6 in.	32.1 in.
Thickness t	2.875 in.	2.875 in.

Using 2.0×10^5 in./sec as the speed of sound in aluminum, we deduce from Eq. (31) that

$\tau_m = 2\pi(18.6)/(2.0 \times 10^5) = 584$ μ sec for the inner coil and $\tau_m = 1.01$ msec for the outer coil.

b. Calculation of the Electrical Period. From previous computer field calculations, the total current (parallel feed) is 1.0 mA when the field energy $\frac{1}{2}LI^2$ is 0.81 MJ. Solving for the total input inductance, we obtain $L = 1.6$ μ H. Using $C = 0.02$ F (1-MJ, 10-kV capacitor bank), the electrical period is $\tau = 2\pi\sqrt{LC} = 1.1$ msec. Hence, $\tau_m/\tau = 0.53$ and 0.91 for the inner and outer coils, respectively.

c. Calculation of Impulse Factors. The τ_m/τ values show that for the oscillatory case the coils are operating in the resonance region of the curves of Fig. 4. Even if the damping allows the current to oscillate about 2 cycles ($\tau/\tau_d = 0.5$), the impulse factor for the rings obtained from Fig. 4 are 2.56 and 1.1. The fortuitous and unfortunate nearness of the inner coil to mechanical resonance is dangerous because small shifts in the parameters

can give even larger peak stresses. If the current is crowbarred at peak field with the estimated damping time of ~ 5 msec, the curves of Fig. 5 apply. Using $\tau_d/\tau = 5$ in Fig. 5, impulse factors of 1.54 and 1.2 are obtained. These results show the danger in designing pulsed systems based on static stresses corresponding to peak field.

d. Static Stress Calculation. The static stresses, S_m , corresponding to field pressures, p , of 40 kG and 25 kG for the inner and outer coils, respectively, can be obtained from the formula

$$S_m = pr/t.$$

Inner coil

$$S_m = (40/5)^2(14.7)(18.6)/(2.875) = 6100 \text{ psi}$$

Outer coil

$$S_m = (25/5)^2(14.7)(32.1)/2.875 = 4100 \text{ psi.}$$

e. Pulsed Stresses. When the static stresses are multiplied by the impulse factors just computed we find that the most critical element is the inner coil at a peak stress under noncrowbarred conditions of $6100 \times 2.56 = 15,600$ psi, which is under the 35,000 psi yield strength of the aluminum to be used. For the two-turn coil actually used, the minimum cross section becomes smaller and the design is more marginal.

REFERENCES

1. G. A. Sawyer and E. L. Zimmerman, private communication.
2. R. V. Churchill, Operational Mathematics, (McGraw Hill Book Company, New York 1958).
3. R. S. Dike, private communication.

APPENDIX: IMPULSE APPROXIMATION

A. Force Due to a Damped Sinusoidal Field

We first compute the total impulse

$$I = \int_0^{\infty} f(t) dt, \quad (A1)$$

where $f(t)$ is given by Eq. (10). The total impulse is then given by

$$I = f_m \int_0^{\infty} e^{-2t/\tau_d} \sin^2 \frac{2\pi}{\tau} t dt, \\ = \frac{f_m}{2} \left[\frac{\tau_d}{2} - \frac{2/\tau_d}{\frac{4}{\tau_d^2} + \frac{16\pi^2}{\tau^2}} \right]. \quad (A2)$$

Simplifying, we have

$$I = \left(\frac{f_m \tau_d}{4} \right) \left(\frac{4\pi^2 \tau_d^2}{\tau^2 + 4\pi^2 \tau_d^2} \right). \quad (A3)$$

The velocity just after the impulse is now computed by setting the change of momentum Δp equal to the impulse

$$\Delta p = mv = I, \quad (A4)$$

where

m = mass of spring,
 v = velocity of the spring just after the impulse;

hence,

$$v = \frac{I}{m}. \quad (A5)$$

We use conservation of energy to set the potential energy of the spring at the time of maximum displacement equal to the initial kinetic energy,

or

$$\frac{1}{2}mv^2 = \frac{1}{2}kx_{\max}^2,$$

where k is the spring constant. Thus, using Eq.

(A5),

$$x_{\max} = v\sqrt{m/k} = \frac{v}{\omega} = I/m\omega, \quad (A6)$$

where $\omega \equiv \sqrt{k/m}$. The static displacement, due to a

force f_m , is

$$x_{\text{static}} = f_m/k. \quad (A7)$$

Combining Eqs. (A6), (A7), and (A3) we obtain the impulse factor

$$X_{\max} = \frac{x_{\max}}{x_{\text{static}}} = \frac{\tau_d}{4} \left[\frac{4\pi^2 \tau_d^2}{\tau^2 + 4\pi^2 \tau_d^2} \right] \omega. \quad (A8)$$

Since $\tau_m \equiv \frac{2\pi}{\omega}$, the impulse factor may be written in the following dimensionless form.

$$X_{\max} = \frac{2}{(\tau/\tau_d)(\tau_m/\tau)} \left[\frac{\pi^3}{(\tau/\tau_d)^2 + 4\pi^2} \right] \quad (A9)$$

B. Force Due to a Crowbarred Field Waveform

Using Eq. (A1) and Eqs. (12) and (13) for this case, we have

$$I = f_m \left[\int_0^{\tau/4} \sin^2 \frac{2\pi}{\tau} t dt + \int_{\tau/4}^{\infty} e^{-2(t-\tau/4)/\tau_d} dt \right],$$

or

$$I = \frac{f_m}{2} \left(\frac{\tau}{4} + \tau_d \right).$$

Proceeding in a similar fashion as before, we get the impulse factor

$$X_{\max} = \frac{x_{\max}}{x_{\text{static}}} = \frac{\pi}{\tau_m} \left[\frac{\tau}{4} + \tau_d \right] = \frac{\pi}{(\tau_m/\tau)} \left[\frac{1}{4} + \frac{\tau_d}{\tau} \right].$$